Available online at www.sciencedirect.com
ScienceDirect
International Journal of Non-Linear Mechanics 43 (2008) 320 – 327
INTERNATIONAL JOURNAL OF NON-LINEAR MECHANICS
www.elsevier.com/locate/nlm

# Autoparametric quasiperiodic excitation

Si Mohamed Sah[b], Geoffrey Recktenwald[a], Richard Rand[a,*], Mohamed Belhaq[b]

[a]*Department of Theoretical and Applied Mechanics, Cornell University, Ithaca NY, USA*
[b]*Faculty of Sciences Aïn Chock, BP 5366 Maârif, Casablanca, Morocco*

Received 3 December 2007; received in revised form 10 December 2007; accepted 19 December 2007

**Abstract**

The dynamics of an autonomous conservative three degree of freedom system which exhibits autoparametric quasiperiodic excitation is investigated. The system is a generalization of a classical system known as the "particle in the plane". The system exhibits a motion, the $z=0$ mode, whose stability is governed by a linear second order ODE with quasiperiodic coefficients. The behavior of the latter ODE is studied by using three different methods: numerical integration, harmonic balance and perturbation methods.


*Keywords:* Parametric resonance; Quasiperiodic; Perturbations

## 1. Introduction

Parametric excitation is a phenomenon associated with systems involving differential equations with periodic coefficients. The paradigm example is Mathieu's equation

$$\ddot{x} + (\delta + \varepsilon \cos t)x = 0. \tag{1}$$

Systems with periodic coefficients typically occur in two different ways. On the one hand they occur in non-autonomous systems which involve periodic forcing. An example is the motion of a pendulum whose support is periodically forced in a vertical direction. The presence of an external forcing function is, however, not required for parametric excitation. A second class of problems involving parametric excitation involves autonomous systems which exhibit periodic motions. In this case a study of the stability of the periodic motion leads to a differential equation with periodic coefficients, a situation referred to as autoparametric excitation [1].

This type of system may be illustrated by an example which will be important to us in the present paper. The example is called the "particle in the plane" and was first studied by Rosenberg and his associates in the 1960s [2–6]. This consists of a particle of unit mass which is constrained to move in the $x$–$y$ plane, and is restrained by two linear springs, each with spring constant of $\frac{1}{2}$. The anchor points of the two springs are located on the $x$-axis at $x = 1$ and $-1$. Each of the two springs has unstretched length $a$. See Fig. 1.

This autonomous two degree of freedom system exhibits an exact solution corresponding to a mode of vibration in which the particle moves along the $x$-axis:

$$x = R\cos t, \quad y = 0. \tag{2}$$

In order to determine the stability of this motion, one must first derive the equations of motion, then substitute $x = R\cos t + u$, $y = 0 + v$, where $u$ and $v$ are small deviations from the motion (2), and then linearize in $u$ and $v$. The result is two linear differential equations on $u$ and $v$. The $u$ equation turns out to be the simple harmonic oscillator, and cannot produce instability. The $v$ Equation is [7]

$$\frac{d^2 v}{dt^2} + \left(\frac{1 - a - R^2\cos^2 t}{1 - R^2\cos^2 t}\right) v = 0. \tag{3}$$

Here stability is defined by all solutions being bounded. An equation is said to be unstable if an unbounded solution exists.

* Corresponding author.
*E-mail address:* rhr2@cornell.edu (R. Rand).

0020-7462/$ - see front matter 
doi:10.1016/j.ijnonlinmec.2007.12.015

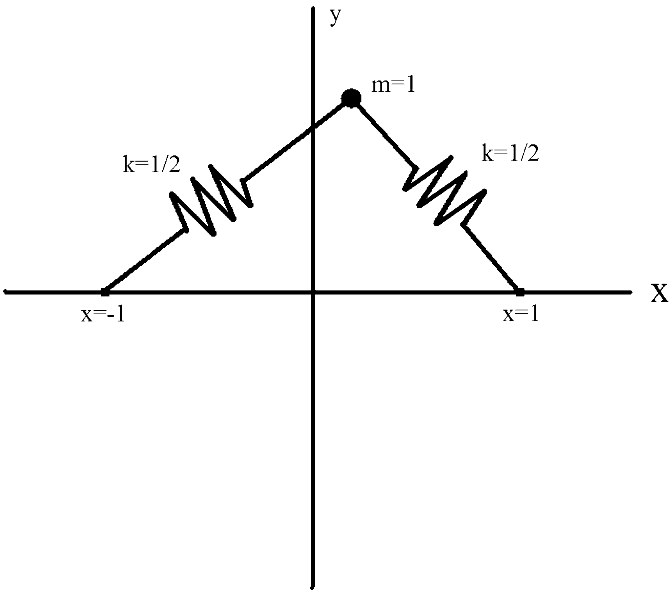


Fig. 1. The particle in the plane consists of a particle of unit mass which is constrained to move in the $x$–$y$ plane, and is restrained by two linear springs, each with spring constant of $\frac{1}{2}$. The anchor points of the two springs are located on the $x$-axis at $x = 1$ and $-1$. Each of the two springs has unstretched length $a$.

The present work involves quasiperiodic parametric excitation, that is, systems which involve differential equations with quasiperiodic coefficients. Here the system which is comparable to Mathieu's equation (1) has been called the quasiperiodic Mathieu equation [8–16]:

$$\ddot{x} + (\delta + \varepsilon \cos t + \varepsilon \cos \omega t)x = 0. \tag{4}$$

Our goal in this paper is to investigate a system which exhibits autoparametric quasiperiodic excitation, that is, an autonomous system which possesses a quasiperiodic motion, the stability of which leads to a differential equation with quasiperiodic coefficients.

## 2. Description of system

The system which we study in this paper has 3 degrees of freedom and is autonomous. It involves a single particle of unit mass restrained by four linear springs and is a generalization of the particle in the plane. Each of the four springs has one end attached to the particle, and the other end attached to a frictionless movable anchor which permits free motion in a direction perpendicular to the length of the spring. The anchors, respectively, run along the lines $x = \pm 1$ and $y = \pm 1$ in the plane $z = 0$. See Fig. 2. As a result of the frictionless movable anchors, the $y$-location of the anchors which run along $x = \pm 1$ are both equal to each other and to the $y$-location of the particle. Similarly for the $x$-location of the anchors which run along $y = \pm 1$.

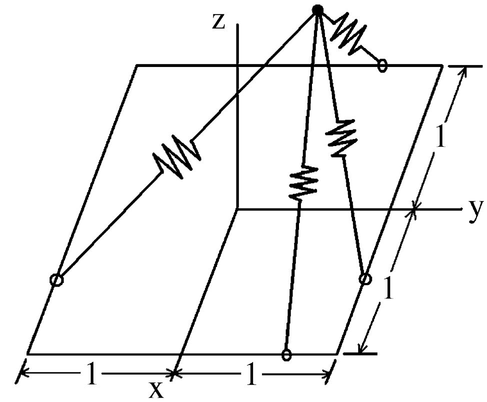


Fig. 2. Three degree of freedom system studied in this paper. A particle of unit mass is restrained by four linear springs and is a generalization of the particle in the plane, cf. Fig. 1. Each of the four springs has one end attached to the particle, and the other end attached to a frictionless movable anchor which permits free motion in a direction perpendicular to the length of the spring. The anchors, respectively, run along the lines $x = \pm 1$ and $y = \pm 1$ in the plane $z = 0$.

The springs all have unstretched length $a$, so that the potential energy is given by

$$V(x, y, z) = \frac{k_x\left(\sqrt{z^2 + (x+1)^2} - a\right)^2}{2} + \frac{k_x\left(\sqrt{z^2 + (1-x)^2} - a\right)^2}{2} + \frac{k_y\left(\sqrt{z^2 + (y+1)^2} - a\right)^2}{2} + \frac{k_y\left(\sqrt{z^2 + (1-y)^2} - a\right)^2}{2}, \tag{5}$$

where $k_x$ and $k_y$ are linear spring constants. The kinetic energy is given by

$$T = \frac{1}{2}\left[\left(\frac{\mathrm{d}z}{\mathrm{d}t}\right)^2 + \left(\frac{\mathrm{d}y}{\mathrm{d}t}\right)^2 + \left(\frac{\mathrm{d}x}{\mathrm{d}t}\right)^2\right]. \tag{6}$$

The system has the following three equations of motion:

$$\frac{\mathrm{d}^2 x}{\mathrm{d}t^2} + \frac{w_x^2(x+1)\left(\sqrt{z^2 + (x+1)^2} - a\right)}{2\sqrt{z^2 + (x+1)^2}} - \frac{w_x^2(1-x)\left(\sqrt{z^2 + (1-x)^2} - a\right)}{2\sqrt{z^2 + (1-x)^2}} = 0, \tag{7}$$

$$\frac{\mathrm{d}^2 y}{\mathrm{d}t^2} + \frac{w_y^2(y+1)\left(\sqrt{z^2 + (y+1)^2} - a\right)}{2\sqrt{z^2 + (y+1)^2}} - \frac{w_y^2(1-y)\left(\sqrt{z^2 + (1-y)^2} - a\right)}{2\sqrt{z^2 + (1-y)^2}} = 0, \tag{8}$$

$$\frac{d^2z}{dt^2}+\frac{w_y^2z\left(\sqrt{z^2+(y+1)^2}-a\right)}{2\sqrt{z^2+(y+1)^2}}+\frac{w_y^2z\left(\sqrt{z^2+(1-y)^2}-a\right)}{2\sqrt{z^2+(1-y)^2}}+\frac{w_x^2z\left(\sqrt{z^2+(x+1)^2}-a\right)}{2\sqrt{z^2+(x+1)^2}}+\frac{w_x^2z\left(\sqrt{z^2+(1-x)^2}-a\right)}{2\sqrt{z^2+(1-x)^2}}=0, \tag{9}$$

where $w_x^2=2k_x$ and $w_y^2=2k_y$.

We note that $z=0$ is an exact solution to Eqs. (7)–(9) corresponding to the invariant manifold $\{z=0, dz/dt=0\}$, which is four dimensional. The motion in this invariant manifold, which we shall refer to as the "$z=0$ mode", is given by

$$\frac{d^2x}{dt^2}+w_x^2x=0, \tag{10}$$

$$\frac{d^2y}{dt^2}+w_y^2y=0. \tag{11}$$

The $z=0$ mode thus has the solution:

$$x=R_x\cos(w_xt), \quad y=R_y\cos(w_yt+\psi), \tag{12}$$

where $\psi$ represents the difference in phase between the $x$ and $y$ motions.

In order to investigate the stability of the $z=0$ mode, we set

$$x=R_x\cos(w_xt)+u, \quad y=R_y\cos(w_yt+\psi)+w, \quad z=0+v \tag{13}$$

and linearize in $u$, $w$ and $v$. This turns out to give that $u$ and $w$ satisfy simple harmonic oscillator equations, and are therefore stable, whereas $v$ satisfies the following equation:

$$\frac{d^2v}{dt^2}+f(t)v=0, \tag{14}$$

where

$$f(t)=\frac{(w_x^2+w_y^2)x^2y^2-((1-a)w_y^2+w_x^2)x^2-((1-a)w_x^2+w_y^2)y^2+(1-a)(w_x^2+w_y^2)}{(x^2-1)(y^2-1)} \tag{15}$$

in which $x$ and $y$ are given by Eq. (12). For general values of $w_x$ and $w_y$, $f(t)$ is quasiperiodic. In what follows, we take $w_x=1$. This is equivalent to stretching time and can be done without loss of generality in this autonomous system.

## 3. Numerical integration

In this section we present stability charts for the $z=0$ mode, obtained by numerically integrating Eq. (14). In the case that the ratio $w_y/w_x$ is irrational, the function $f(t)$ in Eq. (15) will not be periodic, and Eq. (14) will not be treatable by using Floquet theory. However, since an irrational number can be approximated to any order of accuracy by a rational number, we may obtain an accurate representation of the stability chart by sampling only points which correspond to rational values of the ratio $w_y/w_x$. With this sampling technique the parametric forcing function $f(t)$ is periodic allowing us to use Floquet theory.

The stability of the system is found by creating a fundamental solution matrix. The differential equation (14) is numerically integrated for exactly one period of the parametric forcing function $f(t)$, using two sets of initial conditions:

$$\begin{bmatrix} v_1(0) \\ v_{1,t}(0)\end{bmatrix}=\begin{bmatrix}1\\0\end{bmatrix} \quad \text{and} \quad \begin{bmatrix} v_2(0) \\ v_{2,t}(0)\end{bmatrix}=\begin{bmatrix}0\\1\end{bmatrix}. \tag{16}$$

The results are combined into a fundamental solution matrix $C$ whose eigenvalues determine stability:

$$C=\begin{bmatrix} v_1(T) & v_2(T) \\ v_{1,t}(T) & v_{2,t}(T)\end{bmatrix}. \tag{17}$$

If, for a given point in parameter space, either eigenvalue of $C$ has absolute value greater than unity, then that point is said to be unstable (and stable otherwise).

To create Fig. 3 we sampled all frequencies such that $w_y/w_x=m/n$ is rational with $m$ and $n$ relatively prime integers, and where $n<150$ and $0<m/n<2$. In the case that $w_x=1$, the period $T$ is given by the expression $T=2\pi n$. The maximum period sampled is $T=300\pi$. However, portions of the parameter space were carefully swept with $n<1500$ to fill in gaps left by the method.

We set $R_x=e$, $R_y=e$, $w_x=1$, and $\psi=0$ in Eqs. (12). Here $e$ is a parameter which measures the amplitude of the $x$ and $y$ motions. Figs. 3 and 4 show stability charts in the $a$–$w_y$ parameter plane for $e^2=0.5$ and 0.1, respectively.

## 4. Harmonic balance

In order to obtain an analytical approximation for the transition curves in Eq. (14), we use a scheme based on Fourier series known as harmonic balance. This approach was used successfully on Eq. (4) by Zounes and Rand [8]. The idea is to look for solutions along the transition curves in the form

$$v=\sum_{n=0}^{\infty}\sum_{m=-\infty}^{\infty}A_{nm}\cos(nw_x+mw_y)t+B_{nm}\sin(nw_x+mw_y)t \tag{18}$$

in which we take $w_x=1$ without loss of generality. The argument for the above ansatz is made when $w_y$ is restricted to rational values: $w_y=p/q$, where $p$ and $q$ are relatively prime, positive integers. Note that any irrational number can be approximated by a rational number to any degree of accuracy. With this restriction, the Eq. (15) becomes Hill's equation with frequencies $2w_x=2$ and $2w_y=2p/q$ (since $f(t)$ in Eq. (15) depends on $x^2$ and $y^2$, cf. Eq. (12)). In this case $f(t)$ has period $T=\pi q$. According to Floquet theory, any solution $v(t)$ along the transition curves of Eq. (14) has minimum period $2T$ or $4T$, and hence, can be expanded in

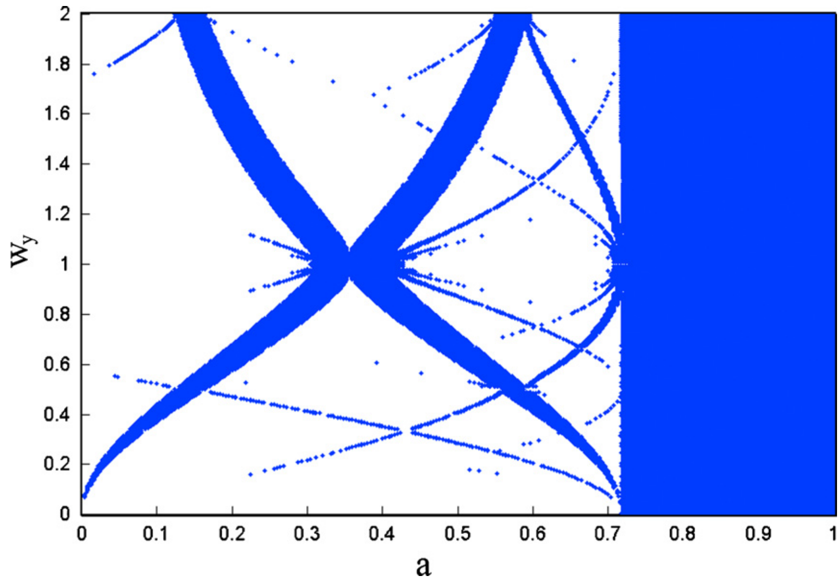


Fig. 3. Stability chart for $z=0$ mode obtained by numerical integration of Eq. (14) for $e^2=0.5$. White regions are stable, black regions are unstable.

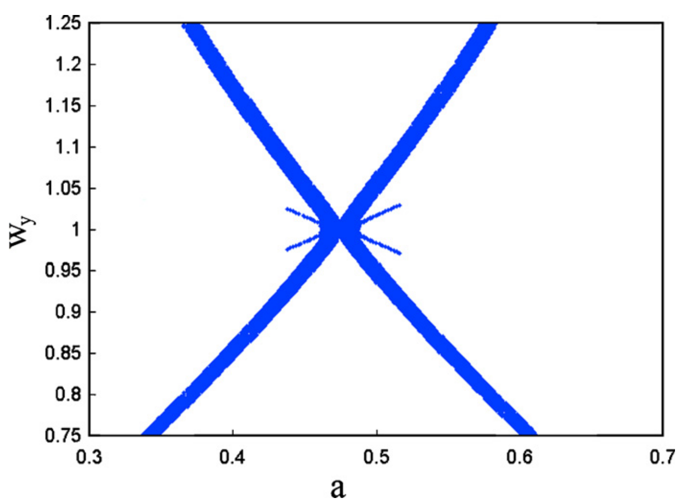


Fig. 4. Stability chart for $z=0$ mode obtained by numerical integration of Eq. (14) for $e^2=0.1$. White regions are stable, black regions are unstable.

a Fourier series:

$$v = A_0 + \sum_{k=1}^{\infty} A_k \cos\frac{k}{q}t + B_k \sin\frac{k}{q}t. \tag{19}$$

Since $p$ and $q$ are relatively prime, any integer $k$ can be expressed as a linear combination $k=nq+mp$. As a result, the set of integers $k$ can be put into a one-to-one correspondence with the set of ordered pairs of integers $\mathscr{I}=(n,m)$. Ordered pairs that yield the same integer are identified and thus the Fourier series (19) can be expressed as follows:

$$\begin{aligned} v &= \sum_{\mathscr{I}} A_{nm}\cos\left(\frac{nq+mp}{q}t\right) + B_{nm}\sin\left(\frac{nq+mp}{q}t\right) \\ &= \sum_{\mathscr{I}} A_{nm}\cos(n+mw_y)t + B_{nm}\sin(n+mw_y)t, \end{aligned} \tag{20}$$

which is in the form of the ansatz given by Eq. (18).

In practice, approximate results are obtained when the infinite sums in Eq. (18) are replaced by sums from 0 to $N$ and from $-N$ to $N$, respectively. Since the forcing term $f(t)$ in Eq. (14) is an even function of $t$, the solution space can be spanned by an even solution and an odd solution. This permits us to take first $B_{nm}$ and then $A_{nm}$ as zero in Eq. (18), thereby reducing the size of the (truncated) determinant by half. In the former case, we substitute Eq. (18) with $B_{nm}=0$ into Eq. (14). Using computer algebra, we perform a trigonometric reduction and collect terms to give the system of $2N^2+2N+1$ simultaneous equations on the $A_{nm}$ only. For example, in the case of $N=3$, the matrix of coefficients has dimension 25. Fig. 5 shows both the sine and cosine solutions for $N=3$, and for parameters $e^2=0.5$, $R_x=e$, $R_y=e$, $w_x=1$, and $\psi=0$. This figure is to be compared with Fig. 3 which was obtained by numerical integration.

Although the expressions for the transition curves in Fig. 3 for $N=3$ are too long to give here, we list the following four transition curves for the case $N=1$. These are displayed in Fig. 6 for comparison with results obtained by the other methods:

$$a = -\frac{(e^2-2)(3e^2-4)w_y^2}{2(3e^2w_y^2-4w_y^2+2e^2-4)}, \tag{21}$$

$$a = -\frac{(e^2-2)(3e^2-4)}{2(2e^2w_y^2-4w_y^2+3e^2-4)}, \tag{22}$$

$$a = -\frac{(e^2-4)(e^2-2)w_y^2}{2(e^2w_y^2-4w_y^2+2e^2-4)}, \tag{23}$$

$$a = -\frac{(e^2-4)(e^2-2)}{2(2e^2w_y^2-4w_y^2+e^2-4)}. \tag{24}$$

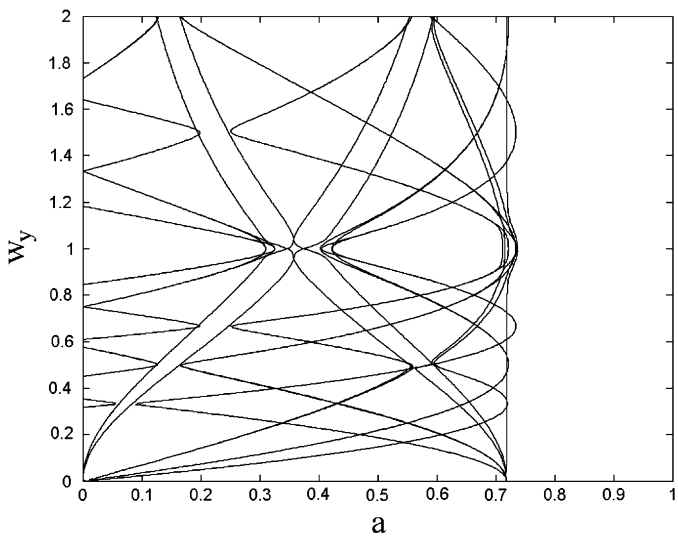


Fig. 5. Transition curves in stability chart for $z=0$ mode obtained by harmonic balance with $N=3$ for $e^2=0.5$. Compare with Fig. 3.

## 5. Perturbation method

In this section we use a perturbation method to investigate the stability of the $z=0$ mode in the case of 1:1:1 resonance. We begin by scaling $x$, $y$ and $z$ in Eqs. (7)–(9):

$$x=\sqrt{e}\hat{x}, \quad y=\sqrt{e}\hat{y}, \quad z=\sqrt{e}\hat{z}, \tag{25}$$

where $e$ is a small parameter, and then dropping the hats for convenience:

$$\frac{d^2x}{dt^2}+w_x^2x-a\,w_x^2xz^2e+\cdots=0, \tag{26}$$

$$\frac{d^2y}{dt^2}+w_y^2y-aw_y^2yz^2e+\cdots=0, \tag{27}$$

$$\frac{d^2z}{dt^2}+(1-a)(w_y^2+w_x^2)z - \frac{(2az(w_x^2x^2+w_y^2y^2)-a(w_x^2+w_y^2)z^3)e}{2}+\cdots=0, \tag{28}$$

where we have neglected terms of $O(e^2)$. Next we choose parameters to produce a 1:1:1 resonance:

$$w_x=1, \quad w_y=\sqrt{1+ek}, \quad a=\tfrac{1}{2}+e\delta. \tag{29}$$

Substitution of Eqs. (29) into Eqs. (26)–(28) shows that each of the oscillators has a linear frequency of unity:

$$\frac{d^2x}{dt^2}+x-\frac{z^2xe}{2}+\cdots=0, \tag{30}$$

$$\frac{d^2y}{dt^2}+y+\frac{(2k-z^2)ye}{2}+\cdots=0, \tag{31}$$

$$\frac{d^2z}{dt^2}+z+\frac{(z^3+(-4\delta+k-x^2-y^2)z)e}{2}+\cdots=0. \tag{32}$$

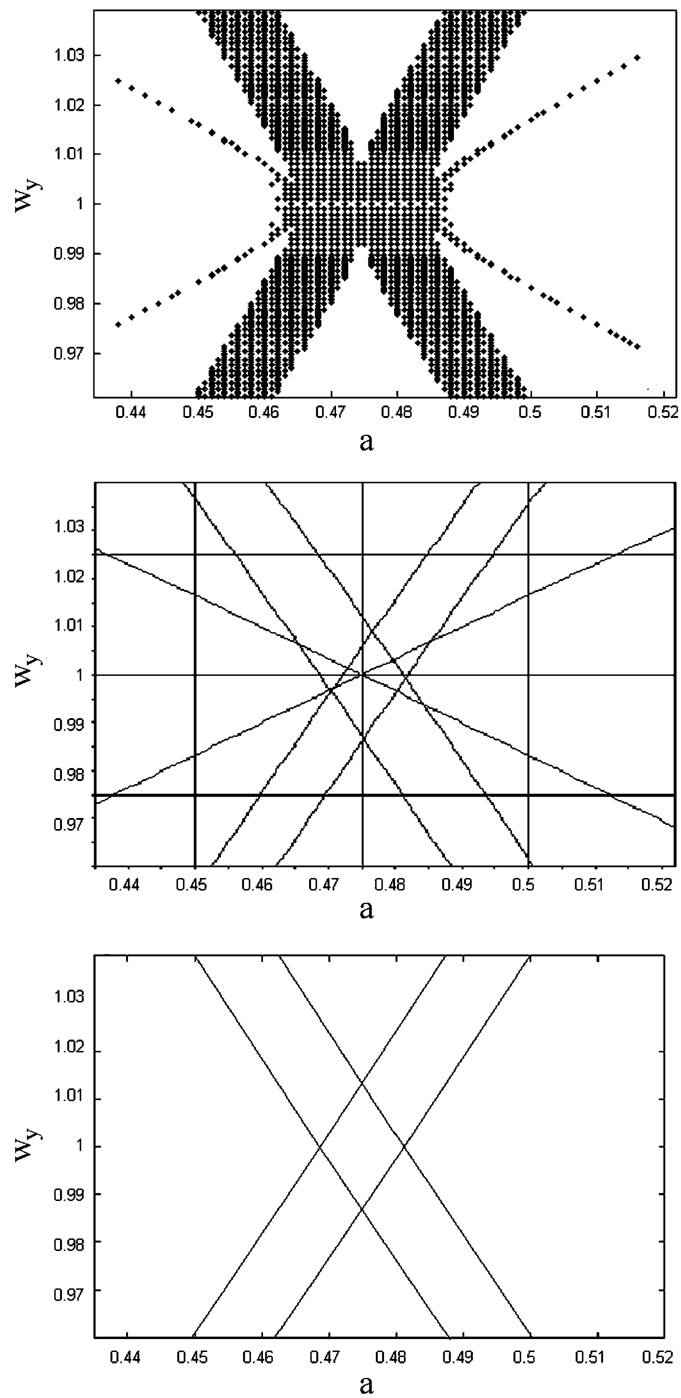


Fig. 6. Comparison of stability chart for $z=0$ mode obtained by numerical integration (top) with transition curves (59)–(64) obtained by perturbations (middle) and transition curves (21)–(24) obtained by harmonic balance with $N=1$ (bottom), all for $e^2=0.1$.

Next we apply the two variable expansion perturbation method [7,17], also known as multiple scales [18], to Eqs. (30)–(32). We set $\xi=t$ and $\eta=et$ (slow time) and we expand

$$x=x_0+ex_1+\cdots, \quad y=y_0+ey_1+\cdots, \\ z=z_0+ez_1+\cdots. \tag{33}$$

Substitution of Eqs. (33) into Eqs. (30)–(32) and collecting terms gives the following equations on $x_0$, $y_0$ and $z_0$:

$$\frac{d^2x_0}{d\xi^2}+x_0=0,\quad \frac{d^2y_0}{d\xi^2}+y_0=0,\quad \frac{d^2z_0}{d\xi^2}+z_0=0 \tag{34}$$

and the following equations on $x_1$, $y_1$ and $z_1$:

$$2\frac{d^2x_1}{d\xi^2}+2x_1=-4\frac{d^2x_0}{d\eta d\xi}+z_0^2x_0, \tag{35}$$

$$2\frac{d^2y_1}{d\xi^2}+2y_1=-4\frac{d^2y_0}{d\eta d\xi}+y_0z_0^2-2ky_0, \tag{36}$$

$$2\frac{d^2z_1}{d\xi^2}+2z_1=-4\frac{d^2z_0}{d\eta d\xi}+z_0x_0^2-z_0^3-(-4\delta-y_0^2+k)z_0. \tag{37}$$

We take the solution to Eqs. (34) in the form

$$x_0=b_x\sin\xi+a_x\cos\xi,\quad y_0=b_y\sin\xi+a_y\cos\xi,$$
$$z_0=b_z\sin\xi+a_z\cos\xi, \tag{38}$$

where $a_x$, $b_x$, $a_y$, $b_y$, $a_z$ and $b_z$ are slowly varying functions of slow time $\eta$. Substituting (38) into Eqs. (35)–(37) and removing secular terms, we obtain the following slow flow:

$$\frac{da_x}{d\eta}=-\frac{3b_xb_z^2+2a_xa_zb_z+a_z^2b_x}{16}, \tag{39}$$

$$\frac{db_x}{d\eta}=\frac{a_xb_z^2+2a_zb_xb_z+3a_xa_z^2}{16}, \tag{40}$$

$$\frac{da_y}{d\eta}=-\frac{-8b_yk+3b_yb_z^2+2a_ya_zb_z+a_z^2b_y}{16}, \tag{41}$$

$$\frac{db_y}{d\eta}=\frac{-8a_yk+a_yb_z^2+2a_zb_yb_z+3a_ya_z^2}{16}, \tag{42}$$

$$\frac{da_z}{d\eta}=-\frac{b_z(-4k+16\delta+3b_y^2+3b_x^2-3a_z^2+a_y^2+a_x^2)-3b_z^3+2a_ya_zb_y+2a_xa_zb_x}{16}. \tag{43}$$

$$\frac{db_z}{d\eta}=\frac{a_z(-4k+16\delta+b_y^2+3a_y^2+3a_x^2)-3a_zb_z^2+(2a_yb_y+2a_xb_x)b_z+a_zb_x^2-3a_z^3}{16}. \tag{44}$$

In order to study the stability of the $z=0$ mode, we linearize Eqs. (39)–(44) in $a_z$ and $b_z$:

$$\frac{da_x}{d\eta}=0,\quad \frac{db_x}{d\eta}=0, \tag{45}$$

$$\frac{da_y}{d\eta}=\frac{b_yk}{2},\quad \frac{db_y}{d\eta}=-\frac{a_yk}{2}, \tag{46}$$

$$\frac{da_z}{d\eta}=\frac{b_zk}{4}-b_z\delta-\frac{3b_y^2b_z}{16}-\frac{3b_x^2b_z}{16}-\frac{a_y^2b_z}{16}-\frac{a_x^2b_z}{16}-\frac{a_ya_zb_y}{8}-\frac{a_xa_zb_x}{8}, \tag{47}$$

$$\frac{db_z}{d\eta}=-\frac{a_zk}{4}+a_z\delta+\frac{a_yb_yb_z}{8}+\frac{a_xb_xb_z}{8}+\frac{a_zb_y^2}{16}+\frac{a_zb_x^2}{16}+\frac{3a_y^2a_z}{16}+\frac{3a_x^2a_z}{16}. \tag{48}$$

We take the solution to Eqs. (45)–(46) in the form

$$a_x=\sqrt{\mu},\quad b_x=0,\quad a_y=\sqrt{\mu}\cos\left(\frac{\eta k}{2}\right),$$
$$b_y=-\sqrt{\mu}\sin\left(\frac{\eta k}{2}\right). \tag{49}$$

Here we have scaled $a_x$, $b_x$, $a_y$ and $b_y$ to go like $\sqrt{\mu}$ in order to use $\mu$ as a small parameter in the analysis of Eqs. (47)–(48). The idea of using perturbations on a slow flow in problems involving quasiperiodic parametric excitation has been used in [14]. We substitute Eqs. (49) into Eqs. (47)–(48) and then differentiate (47) to get a single second order ODE on $a_z$. For convenience in what follows, we replace slow time $\eta$ by slow time $\tau=k\eta$, with the result:

$$(1+h_1\mu)\frac{d^2a_z}{d\tau^2}+h_2\mu\frac{da_z}{d\tau}+(w^2+h_3\mu+h_4\mu^2+h_5\mu^3)a_z=0, \tag{50}$$

where

$$w^2=\left(\frac{1}{4}-\frac{\delta}{k}\right)^2, \tag{51}$$

$$h_1=\frac{\cos\tau-3}{4k-16\delta}, \tag{52}$$

$$h_2=\frac{\sin\tau}{4k-16\delta}, \tag{53}$$

$$h_3=-\frac{(3k+4\delta)\cos\tau+11k-44\delta}{64k^2}, \tag{54}$$

$$h_4=\frac{(k+20\delta)\cos\tau+17k-76\delta}{128k^2(k-4\delta)}, \tag{55}$$

$$h_5=-\frac{\cos(2\tau)-20\cos\tau+43}{1024k^2(k-4\delta)}. \tag{56}$$

The period of the forcing terms in Eq. (50) is $2\pi$, and thus from Floquet theory [7] we know that on the transition surfaces separating stable solutions from unstable solutions in the $\delta$–$k$–$\mu$ parameter space, there are periodic solutions with period $2\pi$ or $4\pi$. Now when $\mu=0$, Eq. (50) becomes $d^2a_z/d\tau^2+w^2a_z=0$, so that the transition curves in the $\delta$–$k$ parameter plane correspond to the condition $w^2=n^2/4$, $n=0,1,2,3,\ldots$, giving

$$\mu=0:\quad \frac{1}{4}-\frac{\delta}{k}=\pm\frac{n}{2},\quad n=0,1,2,3,\ldots. \tag{57}$$

For small $\mu>0$ we may obtain expressions for the transition surfaces in the form

$$\delta=\left(\frac{1}{4}\pm\frac{n}{2}\right)k+\delta_1\mu+\delta_2\mu^2+\cdots \tag{58}$$

by expanding $a_z$ in a power series in $\mu$, substituting into Eq. (50) and choosing the $\delta_i$ coefficients for a periodic solution. The first few expressions so obtained, together with the corresponding values of $n$, are as follows:

$$\delta = \frac{k}{4} - \frac{(\sqrt{22}+22)\mu}{96} + O(\mu^2) \quad (n=0), \tag{59}$$

$$\delta = \frac{k}{4} + \frac{(\sqrt{22}-22)\mu}{96} + O(\mu^2) \quad (n=0), \tag{60}$$

$$\delta = -\frac{k}{4} - \frac{3\mu}{16} + O(\mu^2) \quad (n=1), \tag{61}$$

$$\delta = -\frac{k}{4} - \frac{5\mu}{16} + O(\mu^2) \quad (n=1), \tag{62}$$

$$\delta = \frac{3k}{4} - \frac{\mu}{4} + O(\mu^2) \quad (n=1), \tag{63}$$

$$\delta = -\frac{3k}{4} - \frac{\mu}{4} + O(\mu^2) \quad (n=2). \tag{64}$$

In order to compare these results with the $z=0$ mode stability results presented earlier in this paper, we set $\mu = e$, so that $x$, $y$ and $z$ are $O(e)$, cf. Eqs. (25), (38), (49). Then we may substitute Eqs. (59)–(64) into Eqs. (29) to obtain expressions for $w_y$ and $a$ as functions of $e$. See Fig. 6 which corresponds to $e^2 = 0.1$.

## 6. Conclusions

In this paper we have investigated the dynamics of an autonomous conservative three degree of freedom system which exhibits autoparametric quasiperiodic excitation. The system exhibits a motion, the $z=0$ mode, whose stability is governed by a linear second order ODE with quasiperiodic coefficients. We have studied the behavior of the latter ODE by using three different methods: numerical integration, harmonic balance and perturbation methods. All three methods give a consistent picture of how the stability of the $z=0$ mode depends on the parameters of the problem, namely the frequencies of the $x$ and $y$ motions (as characterized by the ratio $w_y/w_x$) and their amplitudes (assumed equal and represented by $e$). This may be seen by comparing Fig. 3, obtained by numerical integration, with Fig. 5, obtained by harmonic balance. Fig. 6 compares the results obtained by all three methods.

Figs. 3 and 5 show that the stability chart is composed of infinitely many small instability regions. This type of structure has been previously observed in the quasiperiodic Mathieu equation (4) [8]. Although many of the regions are too small to show up in Fig. 3, which was obtained by numerical integration, the method of harmonic balance is able in principle to reveal infinitely many such regions, in the limit as the truncation $N$ goes to infinity. Each instability region may be associated with a distinct resonance between the $x$ and $y$ motions (10), (11) which force the stability Equation (14)–(15) and the $z$ equation (9). This may be seen most clearly in the perturbation approach which results in a study of Eq.(50). Here each instability region is associated with an integer $n$, as in Eq. (57), relating a resonance between $k$, which measures the difference in frequencies between the $x$ and $y$ motions, and $\delta$, which is related to the frequency of the $z$ equation, cf. Eq. (29).

In the numerical simulations we took the phase angle $\psi$ between the $x$ and $y$ motions to be zero, cf. Eq. (12). The reason for this is that the presence of a non-zero value of $\psi$ makes no difference in the stability chart. This has been observed by numerical integration, and can be explained as follows [19]: Eq. (14) is of the form

$$v'' + F(\cos(w_x t), \cos(w_y t + \psi))v = 0. \tag{65}$$

We may write this in the form

$$v'' + F(\cos(p), \cos(q))v = 0 \quad \text{where } p' = w_x \text{ and } q' = w_y. \tag{66}$$

The forcing function $F(\cos(p), \cos(q))$ may be viewed as living on the $p$–$q$ torus. For irrational values of the ratio $w_y/w_x$, the flow on the $p$–$q$ torus is dense, and hence the phase of $q$ relative to $p$ cannot affect boundedness as $t \to \infty$.

## Acknowledgments

Support received from the Moroccan American Commission for Educational and Cultural Exchange through the Fulbright Program is acknowledged by author S.M.S. The hospitality of the Department of Theoretical and Applied Mechanics, Cornell University, is gratefully acknowledged.

## References

[1] N. Minorsky, Nonlinear Oscillations, van Nostrand, Princeton, NJ, 1962.
[2] T.L. Yang, R.M. Rosenberg, On the vibrations of a particle in the plane, Int. J. Non-linear Mech. 2 (1967) 1–25.
[3] T.L. Yang, R.M. Rosenberg, On the forced vibrations of a particle in the plane, Int. J. Non-linear Mech. 3 (1968) 47–63.
[4] R.H. Rand, S.F. Tseng, On the stability of a differential equation with application to the vibrations of a particle in the plane, J. Appl. Mech. 36 (1969) 311–313.
[5] R.H. Rand, S.F. Tseng, On the stability of the vibrations of a particle in the plane restrained by two non-identical springs, Int. J. Nonlinear Mech. 5 (1970) 1–9.
[6] G. Recktenwald, R. Rand, Coexistence phenomenon in autoparametric excitation of two degree of freedom systems, Int. J. Nonlinear Mech. 40 (2005) 1160–1170.
[7] R.H. Rand, Lecture Notes on Nonlinear Vibrations, published on-line by The Internet-First University Press, 2004, ⟨http://dspace.library.cornell.edu/handle/1813/79⟩.
[8] R.S. Zounes, R.H. Rand, Transition curves in the quasiperiodic Mathieu equation, SIAM J. Appl. Math. 58 (1998) 1094–1115.
[9] R. Rand, R. Zounes, R. Hastings, Dynamics of a quasiperiodically forced Mathieu oscillator, in: A. Guran (Ed.), Nonlinear Dynamics: The Richard Rand 50th Anniversary Volume, World Scientific Pub. Co., Singapore, pp. 203–221, 1997 (Chapter 9).
[10] S. Mason, R. Rand, On the torus flow $Y' = A + B \cos Y + C \cos X$ and its relation to the quasiperiodic Mathieu equation, in: Proceedings of the 1999 ASME Design Engineering Technical Conferences, 17th Biennial Conference on Mechanical Vibration and Noise, Las Vegas, NV, September 12–15, 1999, paper no. DETC99/VIB-8052.
[11] R.S. Zounes, R.H. Rand, Global behavior of a nonlinear quasiperiodic Mathieu equation, Nonlinear Dyn. 27 (2002) 87–105.
[12] M. Belhaq, K. Guennoun, M. Houssni, Asymptotic solutions for a damped non-linear quasi-periodic Mathieu equation, Int. J. Non-linear Mech. 37 (2002) 445–460.

[13] K. Guennoun, M. Houssni, M. Belhaq, Quasi-periodic solutions and stability for a weakly damped nonlinear quasiperiodic Mathieu equation, Nonlinear Dyn. 27 (2002) 211–236.
[14] R. Rand, K. Guennoun, M. Belhaq, 2:2:1 resonance in the quasiperiodic Mathieu equation, Nonlinear Dyn. 31 (2003) 367–374.
[15] R. Rand, T. Morrison, 2:1:1 resonance in the quasi-periodic Mathieu equation, Nonlinear Dyn. 40 (2005) 195–203.
[16] N. Abouhazim, R.H. Rand, M. Belhaq, The damped nonlinear quasiperiodic Mathieu equation near 2:2:1 resonance, Nonlinear Dyn. 45 (2006) 237–247.
[17] J.D. Cole, Perturbation Methods in Applied Mathematics, Blaisedell, Waltham, MA, 1968.
[18] A.H. Nayfeh, Perturbation Methods, Wiley, New York, 1973.
[19] R.S. Zounes, R.H. Rand, Transition curves in the quasiperiodic Mathieu equation, in: A.K. Bajaj, N.S. Namachchivaya, M.A. Franchek (Eds.), Nonlinear Dynamics and Controls, DE-Vol. 91, Amer. Soc. Mech. Eng., 1996, pp. 1–6.